Cell Stress and Chaperones (2026) 100149
https://doi.org/10.1016/j.cstres.2026.100149

# Increased FICD-mediated protein AMPylation triggers conserved endoplasmic reticulum stress signaling across species

Mirella A. Hernandez-Lima[1,2] · Blaise L. Mariner[3] · William Giblin[2] · Mark A. McCormick[4] · Matthias C. Truttmann[1,2,5,*]

Received: 13 October 2025 / Revised: 23 January 2026 / Accepted: 4 February 2026


**Abstract**

Post-translational protein modifications (PTMs) are fundamentally important in regulating protein function across species. One such PTM, referred to as protein AMPylation, is increasingly recognized to fine-tune endoplasmic reticulum (ER) stress signaling in metazoans. Protein AMPylation in the ER is catalyzed by conserved fic-domain containing enzymes (fic AMPylases), including FICD (*Homo sapiens*) and FIC-1 (*Caenorhabditis elegans*). However, it remains unclear whether enhanced fic AMPylase-mediated protein AMPylation promotes a conserved cellular response. In this study, we determined the transcriptomic consequences of increased fic AMPylase-mediated protein AMPylation in mouse fibroblasts and young adult nematodes. We find that in *C. elegans*, FIC-1(E274G) over-expression (OE) triggers a unique transcriptional signature, leading to the marked upregulation of pathways involved in cellular stress signaling. We further show that FIC-1(E274G) OE upregulates genes involved in antibacterial innate immune responses and identify a potentially co-regulated gene cluster sensitive to changes in AMPylation levels. Intriguingly, we observe a similar transcriptomic signature in mouse fibroblasts in response to FICD(E234G) OE. A cross-species comparison of the transcriptomes of nematodes, yeast, and mouse fibroblasts enduring increased fic AMPylase-mediated protein AMPylation revealed a conserved transcriptional core response to enhanced AMPylation. Collectively, this study defines a conserved cellular stress response to enhanced fic AMPylase-mediated protein AMPylation.

**Keywords** AMPylation · FICD · BiP · ER stress · UPR

## Introduction

Fic-type AMP transferases (AMPylases/Adenylylases) catalyze the formation of a phosphodiester bond between the hydroxyl group of exposed threonine, tyrosine, and serine residues and the alpha-phosphate of an ATP molecule (AMPylation).[1,2] Using the same catalytic domain, these enzymes are also capable of removing AMP from modified proteins (deAMPylation).[1] Fic AMPylases are critically involved in the regulation of protein homeostasis (proteostasis) in the endoplasmic reticulum (ER) and neurogenesis in metazoans.[1,3–10] One key protein controlled by reversible fic AMPylase-mediated AMPylation is the ER-resident chaperone BiP (HSPA5).[11–14] AMPylation of BiP on Thr518 and/or Thr356 regulates BiP-dependent stress signaling through the unfolded protein response pathway in the ER ($UPR^{ER}$).[15–17] Fic AMPylase knockout mice,[15,17–19] fruit flies (*Drosophila melanogaster*),[4,8] and worms (*Caenorhabditis elegans*)[14,20,21] are viable, but exhibit altered responses to protein unfolding stress. Contrasting, increased fic AMPylase-mediated protein AMPylation is cytotoxic and

* Matthias C. Truttmann
mtruttma@med.umich.edu

1 Neuroscience Graduate Program, University of Michigan, Ann Arbor, MI, 48109, USA

2 Department of Molecular & Integrative Physiology, University of Michigan, Ann Arbor, MI, 48109, USA

3 Center for Evolution and Medicine, Arizona State University, Tempe, AZ 85287-1701, USA

4 School of Medicine, University of New Mexico, Albuquerque, NM, USA

5 Geriatrics Center, University of Michigan, Ann Arbor, MI, 48109, USA.

Published online: 6 February 2026

lethal in *C. elegans* and *D. melanogaster*.[4,14] Consistent with these in vivo phenotypes, the expression of a mutant fic AMPylase, FICD(E234G), which is deficient in deAMPylation activity yet a potent AMP transferase,[6] is cytotoxic in human cells.[11,22] Two recent studies further identified a pair of disease-associated FICD mutations in patients presenting with infancy-onset diabetes and motor neuron degeneration.[23,24] Both mutant enzymes, FICD(R371S) and FICD(R374H) exhibit diminished deAMPylation activity while AMPylation activity is maintained, leading to an accumulation of AMPylated BiP. However, the mechanisms through which enhanced or irreversible protein AMPylation impairs cellular health and reduces organismal fitness remain poorly understood.

In this study, we show that inducible over-expression (OE) of the constitutively active *C. elegans* AMPylase FIC-1(E274G) profoundly alters gene expression in vivo. Using RNA-seq, we find that FIC-1(E274G) OE up-regulates innate immunity genes, causes ER stress, and $UPR^{ER}$ signaling. In a complementary model, we demonstrate that OE of hyperactive FICD(E234G) in mouse embryonic fibroblasts (MEFs) elicits a similar response, with 155 ER stress- and chaperone-related genes strongly induced, while few were suppressed. Finally, we perform cross-species analyses using RNAseq datasets from worm, mouse, and yeast experiencing enhanced fic AMPylase-mediated protein AMPylation. This analysis uncovered a conserved transcriptomic signature marked by elevated expression of ER protein-folding genes (BiP/HSPA5, PDIs, ERO1, ATF4) and reduced expression of genes encoding for metabolic enzymes, establishing increased Fic-mediated AMPylation as an evolutionarily conserved trigger of ER stress programs and metabolic adaptations.

## Results

### Increased FIC-1(E274G)-mediated protein AMPylation up-regulates innate immunity genes in *C. elegans*

Why does increased protein AMPylation lead to significant health impairments across species? We approached this question by RNAseq-based transcriptomics comparing wild type *C. elegans* animals with worms that inducibly OE the constitutively active mutant AMPylase FIC-1(E274G) from allele *nIs774* (Fig. 1a). This allele was previously shown to promote robust FIC-1(E274G) OE within 2 h following induction by a short heat pulse (37°C for 30 min).[1] We analyzed and compared four sample cohorts, each represented in biological triplicates: uninduced N2 wild type, uninduced *nIs774*, induced N2 wild type, and induced *nIs774*. Twelve hours after induction, we extracted total RNA from approximately 2000 synchronized day 1 adult animals per replicate of each of the four sample cohorts. Following RNA quality control checks, we prepared polyA RNAseq libraries, which were run on an Illumina NextSeq sequencer by the Michigan Advanced Genomics core. After aligning the reads to the *C elegans* reference genome, we performed Euclidian distance (Fig. 1b) and principal component analyses (Fig. 1c). In both approaches, we observed four distinct and separated clusters, each consisting of the three replicates per sample. As anticipated, the separation was greatest for samples overexpressing FIC-1(E274G), whereas samples of uninduced N2 wild-type and *nIs774* were most related. Fic-1 wild-type expression from the endogenous locus was low yet detectable in all samples (Figure S1a). We further confirmed FIC-1(E274G) OE and associated increased HSP-3/HSP-4 AMPylation in nematodes biochemically (Figures S1b-S1d). These results suggest that our RNAseq approach was robust and replicable. The spatial separation of the individual clusters further indicates distinct transcriptional fingerprints for each tested condition. Next, we performed differential gene expression analyses, comparing induced *nIs774* samples to each of the three control conditions. We focused our analyses on 12,163 genes, which showed a coverage of at least 5 reads in each sample and replicate (Supplementary Table S1). As expected, FIC-1(E274G) OE resulted in pronounced transcriptional changes. We identified 62 genes that are at least 5-fold up-regulated and 9 genes at least 5-fold down-regulated in induced *nIs774* samples compared to all other samples (Supplementary Table S2). Spot-validation of several genes by qPCR confirmed the results observed in the RNAseq analysis (Figure S1e-f). Gene ontology analysis showed that these up-regulated genes were linked to innate immune responses in *C elegans* (Supplementary Table S3). Next, we performed gene ontology analysis using a ranked list of genes that were at least 3-fold up-regulated in induced *nIs774* compared to induced N2 wild type. We observed a significant enrichment for genes associated with innate immune signaling as well as the $UPR^{ER}$, particularly PERK and IRE-1 mediated signaling (Fig. 1d, Supplementary Table S4). Notably, these changes parallel gene expression differences observed upon *hsp-3* and *hsp-4*—the two *C elegans* BiP orthologs—knockdown,[25] suggesting that AMPylation-mediated BiP inhibition may drive at least some of the observed transcriptional changes. These results suggest that FIC-1(E274G) OE activates the $UPR^{ER}$ and $UPR^{ER}$-associated stress responses, many of which overlap with innate immune signaling in *C elegans*.[26,27] Finally, we used STRING to group the list of genes up-

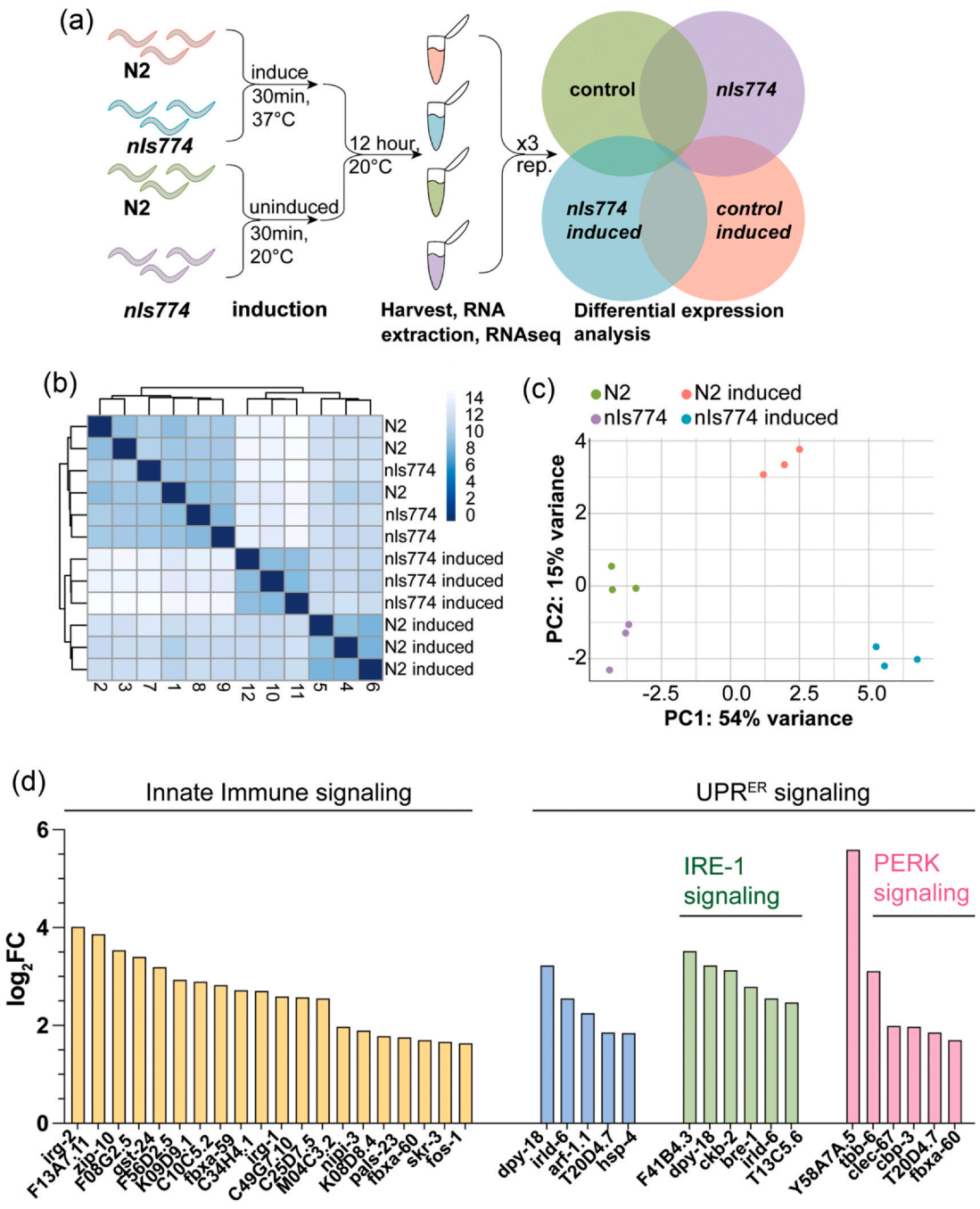


**Fig. 1** *Increased FIC-1(E274G)-mediated AMPylation in C elegans leads to transcriptional upregulation of innate immunity and ER stress genes.* (a) Schematic of the experimental design for RNAseq analysis. Synchronized day 1 adult *C elegans* carrying the FIC-1(E274G) OE transgene (*nIs774*) or wild-type (N2) were subjected to a short heat-pulse induction or maintained at 20 °C as controls. Animals were harvested 12 h post-induction for RNA extraction and transcriptome analysis in biological triplicates. Venn diagram depicts the four experimental groups compared in the study. (b) Sample distance matrix (Euclidean distance heatmap) showing high intra-group similarity and distinct clustering of replicates within each experimental condition, confirming robust gene expression changes upon FIC-1(E274G) overexpression. (c) Principal component analysis (PCA) of RNAseq datasets demonstrates clear separation of the four sample cohorts, with *nIs774*-induced samples forming a distinct cluster characterized by the highest transcriptional divergence. (d) Bar plots displaying $\log_2$ fold changes ($\log_2$FC) of representative genes significantly up-regulated in induced *nIs774*-induced animals versus all three controls. Left: Genes linked to innate immune signaling (yellow). Right: Genes involved in UPR$^{ER}$ signaling, subdivided by IRE-1 (green), PERK (pink), or other ER stress response pathways (blue).

regulated at least 3-fold or 5-fold in induced *nIs774* compared to induced N2 wild type into functional association networks (Figure S2A and b). Consistent with our gene ontology analysis, we observed several functional clusters consisting of genes converging on the innate immunity functions, cell cycle regulation, autophagy, and UPR$^{ER}$ signaling. Taken as a whole, these results implicate a direct link between enhanced FIC-1(E274G)-mediated protein AMPylation and a dysregulation of ER stress signaling, cell division, and innate immunity in *C elegans*.

### Knockdown of major up-regulated genes does not prevent FIC-1(E274G)-induced developmental arrest

FIC-1(E274G) OE during early larval stages leads to developmental arrest.[20] Because impaired innate immune and UPR$^{ER}$ signaling as observed during FIC-1(E274G) OE can trigger apoptosis, we next tested if RNAi-mediated knockdown of significantly up-regulated genes would prevent developmental arrest in FIC-1(E274G) OE larvae. We fed worms with RNAi to knockdown selected genes in N2 wild type, *nIs774*, *uIs60*, and *nIs774;uIs60* animals and tested their F1s in development assays. The allele *uIs60* [*unc-119p*:YFP + *unc-119p*:*sid-1*][28] sensitizes worms to RNAi treatment in neurons, whereas N2 wild-type neurons are largely insensitive to RNAi conditions.[28] Perhaps not surprising, we observed that none of the tested single-gene knockdowns resulted in a significant rescue of larval development upon induction of FIC-1(E274G) OE in either a wild-type or *uIs60* background (Figure S3). These results suggest that the toxicity exerted by FIC-1(E274G) OE is likely the consequence of supraphysiological protein AMPylation and not mediated through the increased transcription of a pro-apoptotic stress-related gene.

### Enhanced FICD(E234G)-mediated protein AMPylation in MEFs activates the ER stress response

In a next step, we addressed the impact of increased AMPylation on gene transcription in immortalized MEF cells. Since the presence of the endogenous wild-type *Ficd* allele prevented FICD(E234G)-mediated increased AMPylation, we used *Ficd* knockout MEFs in which we inducibly expressed either FICD wild type or constitutively active FICD(E234G). Biochemical analysis confirmed robust FICD(E234G) expression and accompanied increases in BiP AMPylation upon induction with doxycycline (Figure S4a-b, S5). Consistent with the results observed in worms, principal component and Euclidian distance analyses showed that the overexpression of the constitutive AMPylase, FICD (E234G) led to significant changes in gene expression (Figure 2a and e). As for the nematode dataset, Spot-validation of several genes by qPCR confirmed the results observed in the RNAseq analysis (Figure 2b-d). Notably, considering genes with a coverage of at least five reads in each sample and replicate, we identified 142 gene that were up-regulated at least four-fold in FICD(E234G) OE MEFs compared to FICD(WT)-expressing cells (Table S5). This suggests that increased FICD-mediated protein AMPylation does not measurably suppress mRNA synthesis and gene transcription. Gene ontology and gene network analysis using STRING indicated that FICD(E234G) expression significantly affected ER stress signaling, chaperone-mediated protein folding, and cellular stress signaling (Figure 2c and S4c). Among the 142 gene up-regulated at least four-fold were several UPR$^{ER}$-associated genes: *Atf3*, *Hspa5*, *Dnajb9*, *Pdia4*, *Manf*, *Ppp1R15A*, *Trib3*, and *Chac1* and *Sel1l*. Notably, the gene products ATF3, PPP1R15A, CHAC1, and TRIB3 are associated with ER stress-mediated cell death, a mechanism increasingly exploited by genotoxic chemotherapy agents in cancer treatment (Figure 3d).[29,30]

### Conserved cross-species signatures of increased AMPylation-mediated transcriptional changes

Are transcriptional responses to increased fic AMPylase-mediated protein AMPylation conserved? To address this question, we first searched for overlap in differential gene expression profiles from the two RNAseq datasets disclosed in this study. Using the Alliance ortholog tool,[31] we first mapped orthologous genes between mouse and worm genomes. We next used a fully linear model to identify genes in our RNAseq datasets that were significantly ($P < 0.05$) up- or down-regulated in both FICD(E234G)-expressing MEFs and FIC-1(E274G)-expressing worms. We identified 104 mouse genes, mapping to 118 *C elegans* genes, that were significantly up- or down-regulated in response to increased AMPylation in both species (Table S6). Gene ontology analysis showed that the conserved differentially regulated genes are associated with protein folding in the ER and amino acid metabolism (Figure 3a). Among the up-regulated genes was BiP (*Hspa5* in mice; *hsp-3* AND *hsp-4* in worms), the ER-resident HSP70 family chaperone and best-described target of FICD/FIC-1[11–13] (Figure 3b). Other notable genes included *Pdia3* and *Pdia4*, encoding for a pair of protein disulfide isomerases that catalyze the formation and breakage for disulfide bonds in ER-resident proteins, *Ero1a* and *Ero1b*, two ER-resident oxidoreductases, and *Atf4*, a transcription factor responsive to the UPR$^{ER}$ and the integrated stress response through interactions with

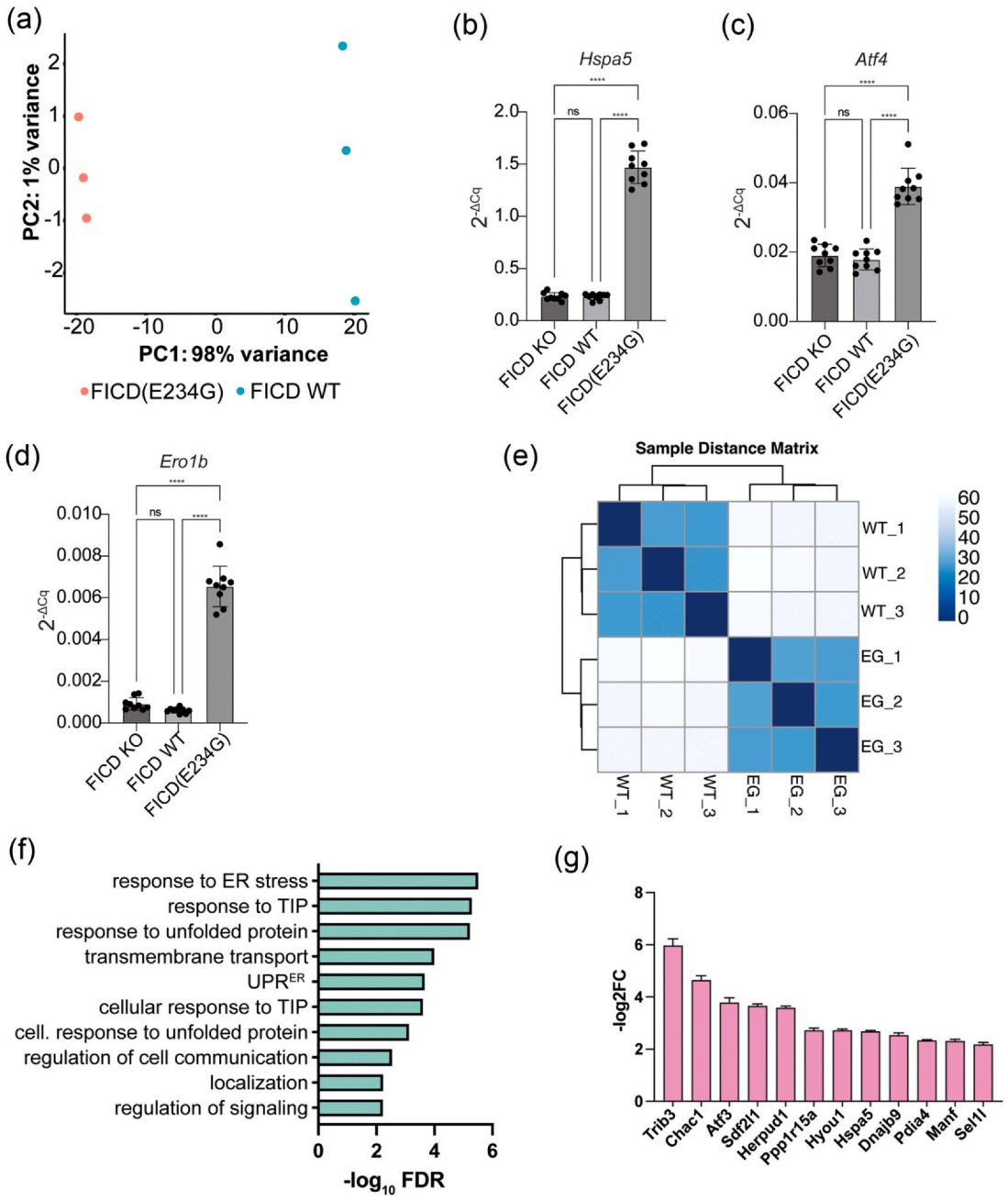


**Fig. 2** *Overexpression of constitutively active FICD(E234G) in MEFs induces gene networks associated with the ER stress response.* (a) Principal component analysis (PCA) of transcriptomes from FICD(E234G)-induced and FICD wild-type (WT) MEFs showing clear clustering and transcriptional reprogramming upon FICD(E234G) induction. (b-d) Quantitative RT-PCR gene expression analysis of *Hspa5* (b), *Atf4* (c) and *Ero1b* (d) in *Ficd* KO, *Ficd* WT, and FICD(E234G) cells. Error bars represent standard deviations. Significance calculated using one-way ANOVA. ****$P < 0.0001$. Graphed mean values represent 3 technical replicates from 3 biological replicates ($n = 9$). (E) Sample distance matrix (Euclidean distances) highlighting robust intra-group clustering and large transcriptional divergence between FICD(WT) and FICD(E234G) MEFs. (f) Gene ontology (GO) analysis for at least four-fold up-regulated genes in FICD(E234G)-overexpressing MEFs revealing enrichment for ER stress response, unfolded protein response ($UPR^{ER}$), and related processes. (g) Bar plot showing $\log_2$ fold change ($\log_2$FC) in expression of selected up-regulated genes (all with adjusted $P < 0.05$), many of which are hallmarks of ER stress, $UPR^{ER}$ signaling, and ER stress-mediated cell death (*e.g., Trb3, Chac1, Atf3, Pdia4, Manf, Sel1l*).

phosphorylated EIF2alpha[32,33] (Figure 3b). In contrast, genes encoding for fatty acid elongase 6 (*Elovl6*), citrate synthase (*Cs*), stearoyl-CoA desaturase 1 (*Scd1*), succinate-CoA ligase (*Suclg1*), and glutamate dehydrogenase (*Glud1*) were significantly down-regulated in both MEFs and *C elegans* cells (Figure 3b).

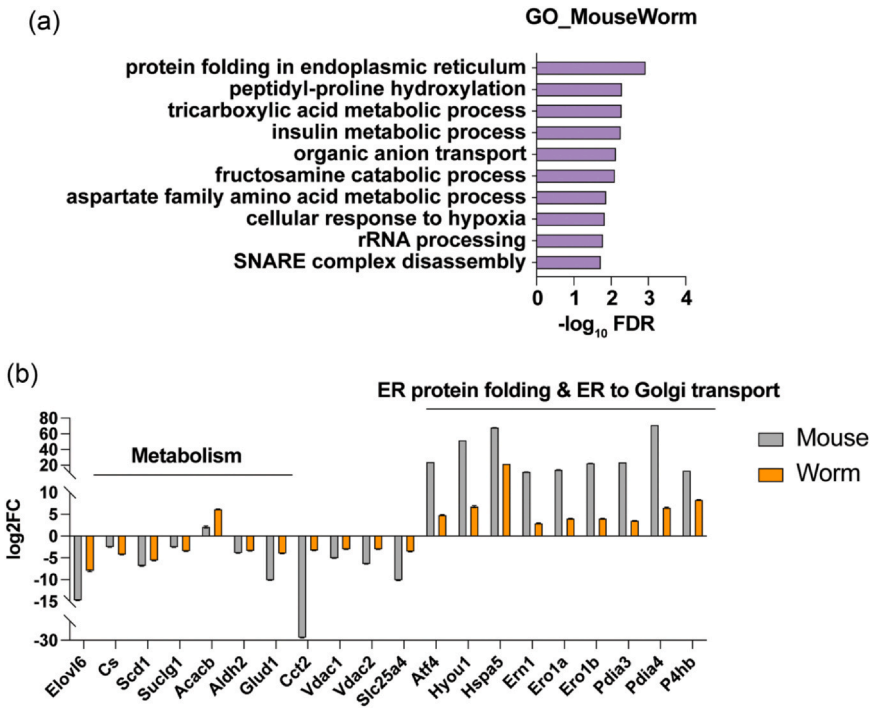


**Fig. 3** *Conserved transcriptomic signatures of enhanced AMPylation across C elegans and mouse.* (a) Gene ontology (GO) enrichment analysis for 104 mouse genes (corresponding to 118 orthologs in *C elegans*) differentially expressed in both FICD(E234G)-expressing MEFs and FIC-1(E274G)-expressing worms. Top terms are related to ER protein folding and various metabolic processes. (b) Bar plot of $\log_2$ fold changes ($\log_2$FC) for selected conserved genes involved in ER protein folding/ER-to-Golgi trafficking (right) and metabolic genes (left) commonly regulated in both mouse (gray) and worm (orange) in response to increased AMPylation.

In a next step, we repeated this analysis, including a previously published RNAseq dataset of *Saccharomyces cerevisiae* (yeast) cells expressing the constitutively active *C elegans* AMPylase FIC-1(E274G).[21] Unlike most eukaryotes, yeast do not express an endogenous fic-domain containing AMPylase. This offered a unique opportunity to include the yeast RNAseq dataset as an example of how enhanced AMPylation in a cell unfamiliar with protein AMPylation in the ER alters gene expression. Since the yeast dataset consisted of a series of samples collected over a 4-hour period, we treated the 1-, 2-, and 4-hour samples as individual replicates of the combined yeast RNAseq dataset. To induce FIC-1(E274G) OE, yeast cells were treated with galactose. Cells carrying an empty plasmid but induced with galactose in parallel served as reference controls. Using a fully linear model and a cut-off of $P < 0.05$, we identified 13 genes that were differentially regulated in the same direction in response to enhanced protein AMPylation (Figure 4a). Most of these genes, including *Aldh1a7*, *Aldh2*, *Aldh1a1*, *Arrdc2*, *Arrdc4*, and *Cs* were associated with cellular metabolism. Gene ontology analysis indicated that several of the identified 13 genes are associated with cellular aldehyde, fructose, and alcohol metabolism (Figure 4b). Notably, no gene linked to ER stress signaling was among the 13. This is consistent with published results[21] showing that FIC-1(E274G) expression in yeast cells significantly up-regulates the heat shock response but not the UPR$^{ER}$. Taken as a whole, our analysis shows that increased fic protein-mediated protein AMPylation down-regulates genes associated with metabolic processes while upregulating ER stress response genes.

## Discussion

In this study, we present a detailed cross-species transcriptomic assessment of cellular responses to increased protein AMPylation driven by constitutively active fic AMPylases. In *C elegans*, FIC-1(E274G) OE caused marked transcriptional remodeling, promoting the up-regulation of genes associated with the UPR$^{ER}$, ER chaperones, and innate-immunity components, whereas the down-regulated set centered on fatty-acid elongation, citrate synthase, stearoyl-CoA desaturase, and other metabolic enzymes. In MEFs, FICD(E234G) OE up-regulated 155 genes by ≥4-fold, including BiP (*Hspa5*), ATF4 targets, and ER-stress-responsive apoptotic factors, but no significant down-regulated gene were detected.

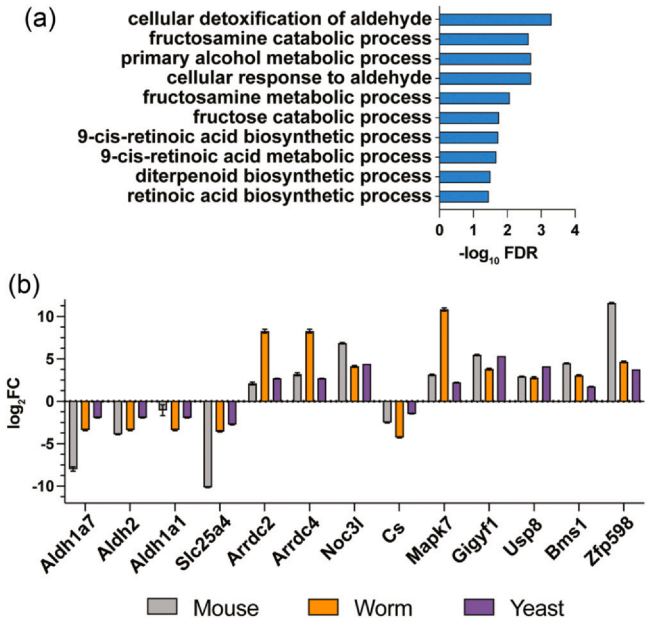


**Fig. 4** *Conserved transcriptomic signatures of increased AMPylation across C elegans, mouse, and yeast species.* (a) Bar plot showing expression changes ($log_2$ fold change) of 13 orthologous genes most consistently up-regulated by increased AMPylation in mouse (grey), worm (orange), and yeast (purple). These genes are primarily involved in aldehyde and alcohol metabolism. (b) GO analysis for the 13 genes up-regulated in response to increased AMPylation in MEFs, worms, and yeast, highlighting enrichment in aldehyde and retinoic acid metabolism.

These results indicate that enhanced AMPylation consistently activates ER- and protein folding stress pathways, consistent with previous studies linking FICD and FIC-1 to the regulation of ER proteostasis.

Ortholog mapping connected 104 mouse genes to 118 *C elegans* orthologs showing concordant differential expression, and gene-ontology analysis highlighted protein-folding, amino-acid metabolism, and ER quality-control functions as shared response elements. Inclusion of yeast, an organism lacking endogenous fic AMPylases, reduced the conserved signature to just 13 genes, all linked to generic aldehyde, fructose, and alcohol metabolism; yeast expressing FIC-1(E274G) failed to elicit canonical $UPR^{ER}$ activation. These findings emphasize that the sensitivity of the ER-stress/innate-immunity axis to increased AMPylation observed in metazoans is not universally conserved and may represent an organismal-specific adaptation to AMPylation imbalance.

Our work does not provide definitive answers as to how increased AMPylation leads to cell death. Our results indicate that the uncontrolled upregulation of ER stress responses leading to ER-mediated cell death may contribute to this process in both MEFs and *C elegans*. Changes in catabolic metabolism upon increased AMPylation may further sensitize cells to cell death. However, it appears most plausible that enhanced fic AMPylase-mediated protein AMPylation interferes with multiple cellular signaling pathways, ultimately culminating in cell death.

### Limitations of this study

The interpretation of our results is complicated by several factors. First, the work relies solely on mRNA sequencing; no protein-level validation, functional assays, or organismal phenotyping was performed to explicitly test connections observed in mRNA signatures. Second, the endogenous *fic-1* wildtype allele was still present in all utilized worm strains; despite its low expression level, it is plausible that trace amounts of wildtype FIC-1 may have slightly reduced/enhanced observed AMPylation levels in all conditions. Third, the temporal resolution of our study is limited, potentially excluding early or late gene expression patterns, complicating interspecies comparisons. Fourth, cross-species analyses depend on imperfect one-to-many ortholog assignments, which can obscure nuanced evolutionary relationships. Nevertheless, our experiments suggest that enhanced protein AMPylation in the ER dysregulates ER-stress signaling and cellular metabolism, leading to cell death.

## Methods

### Mouse embryonic fibroblast isolation and immortalization

*Ficd*$^{-/-}$ MEFs were isolated as described in Durkin et al[2] and immortalized by serial passaging for 8 weeks.

### Lentiviral transduction of *Ficd*$^{-/-}$ MEFs

Previously established lentiviral pInducer plasmids[3] encoding neomycin phosphotransferase II and expressing either wildtype (WT) or p.Glu234Gly (E234G) mutant human FICD under the control of a tetracycline-responsive promoter were used to generate lentiviral particles. Lentiviral FICD plasmids and packaging plasmids (psPAX2, Addgene plasmid #12260 and pMD2. G, Addgene plasmid #12259) were co-transfected into 293T cells using Lipofectamine 2000 (Invitrogen) as previously described.[3] Transfection media was replaced 24 h post-transfection. Viral supernatants were harvested 48 h post-transfection, clarified though a 0.45 μm filter, and applied to immortalized *Ficd*$^{-/-}$ MEFs in the presence of 8 μg/ml polybrene. Fresh growth medium was added to transfected 293T cells after each harvest, collected 24 h later, clarified and

applied to target *Ficd*$^{-/-}$ MEFs. After three rounds of infection, G418 (Gibco) was added to a final concentration of 400 μg/ml 24 h after the final round of infection to select for transductants. Expression of FICD$^{WT}$ and FICD$^{E234G}$ was confirmed via immunoblot 24 h after the addition of 50 ng/ml doxycycline.

### Cell culture and RNA extraction

Human FICD$^{WT}$ and FICD$^{E234G}$ expressing MEFs were cultured in DMEM (Gibco) containing 4.5 g/L glucose, 110 mg/L sodium pyruvate, 4 mM L-glutamine, 100units/ml penicillin (Gibco), 100 μg/ml streptomycin (Gibco), 0.1 mM non-essential amino acids (Gibco), 20 mM HEPES (Gibco), 10% Tet System Approved FBS (Takara), and 100 μM 2-mercaptoethanol (Sigma-Aldrich), while 293T cells were maintained in DMEM (Gibco) containing 4.5 g/L glucose, 110 mg/L sodium pyruvate, 4 mM L-glutamine, 100units/ml penicillin (Gibco), 100 μg/ml streptomycin (Gibco), and 10% heat-inactivated FBS (Corning). All cell lines were routinely confirmed to be free of mycoplasma contamination by PCR and were grown in a humidified chamber at 37 °C containing 5% $CO_2$ and ambient oxygen tension.

MEFs were plated at a density of $1\times10^4$ per well of a 6-well dish 24 h before induction of FICD expression. The following day, culture media were replaced with medium containing 50 ng/ml doxycycline to induce FICD$^{WT}$ or FICD$^{E234G}$ expression. After 24 h in induction media, cells in 3 wells were washed twice with ice-cold PBS and lysed in 1 ml TRIzol Reagent (Invitrogen). RNAs from each of three wells from both FICD$^{WT}$ and FICD$^{E234G}$ were extracted and purified, according to the manufacturer's protocols. RNAs were then treated with 10 units of RNase-free DNAse I (Roche) for 30 min at 37ºC, according to the manufacturer's instructions. RNA integrity was determined by gel electrophoresis. A remaining well was harvested for protein to confirm expression of FICD$^{WT}$ and FICD$^{E234G}$ by immunoblot.

### Transcriptome sequencing of transgenic *Ficd*$^{-/-}$ MEFs

Total DNAse I-treated RNAs from FICD$^{WT}$ (n=3) or FICD$^{E234G}$ ($n$=3) expressing *Ficd*$^{-/-}$ MEFs were submitted to the Novogene Corporation Inc. for sample processing, quality control, and Eukaryotic mRNA Sequencing (NovaSeq X Plus Series; PE150; 6.00G raw data per sample).

### *Caenorhabditis elegans* strains and maintenance

All *C elegans* strains were maintained using standard procedures as described by Brenner (1974). Worms were cultured on nematode growth medium (NGM) agar plates seeded with *Escherichia coli* strain OP50 as the food source. Unless otherwise noted, strains were maintained at 20 °C under standard laboratory conditions. Wild-type worms were of the Bristol N2 strain. Worm strains used in this study are listed in Supplemental Table S7. All strains were obtained from the Caenorhabditis Genetics Center (CGC, University of Minnesota) unless otherwise indicated.

### Worm synchronization

Strains were propagated by chunking, whereby a small agar block containing a mixed-stage population was transferred to a fresh NGM plate seeded with OP50, every 3-4 days, to maintain healthy populations and prevent starvation. All experiments were performed using age-synchronized populations of worms obtained by hypochlorite treatment of gravid adult worms. Worms were collected from NGM plates with water, sedimented, and washed three times with M9 buffer (3 g $KH_2PO_4$, 6 g $Na_2HPO_4$, 5 g NaCl in 950 ml Milli-Q water). Gravid adults were treated with freshly prepared hypochlorite solution (56.6 ml distilled water, 14.4 ml 5N NaOH, 6.6 ml 8.25% NaOCl) and incubated at 20 °C for 7 min with agitation (1200 rpm). Samples were centrifuged at 100 g for 30 s and washed twice with water. Embryos obtained from the hypochlorite treatment were subsequently plated onto RNAi experimental plates.

### RNAi-mediated knockdown experiments

Gene knockdown was achieved using RNA interference (RNAi) by feeding. *C elegans* were exposed to *E coli* HT115 strains expressing small interfering RNA (siRNA) precursors. Bacterial cultures were grown overnight in LB medium supplemented with 100 μg/ml carbenicillin at 37°C, concentrated, and induced with 5 mM isopropyl β-D-1-thiogalactopyranoside (IPTG). NGM plates were supplemented with 100 μg/ml carbenicillin and 1 mM IPTG and seeded with the corresponding RNAi bacteria. HT115 expressing siRNAs targeting *gfp* or *pos-1* served as negative and positive controls, respectively. Knockdown efficiency and target specificity were validated by quantitative PCR (qPCR; data not shown).

### Developmental assays

Eggs were transferred to RNAi plates, and the initial egg count was recorded. Plates were then assigned to one of two groups: a non-heat induction control or a heat-induction treatment. To induce FIC-1 expression, all

animals in the heat-induction group were incubated at 37 °C for 30 min, followed by a 30-min recovery period at 20 °C. Animals in the control group were maintained at 20 °C during this period to prevent unintended FIC-1induction. After recovery, all animals were maintained at 20 °C for 96 h to allow development to adulthood. Following this period, adult worms were counted to assess developmental outcomes.

### *Caenorhabditis elegans* RNAseq sample preparation

For RNAseq sample preparation, we followed a previously established protocol to obtain high-quality *C elegans* mRNA.[25,34] In brief, N2 wild type and *nIs774* animals were synchronized by bleach prepping and grown on standard 100 mm NGM-agar plates seeded with *E coli* OP50. Worms were incubated at 20 °C for 72 h. To induce FIC-1(E274G) OE, *nIs774* animals were incubated at 37 °C for exactly 30 min (referred to as *nIs774* induced). To control for heat-related changes in gene expression, one cohort of N2 wild-type animals was exposed to the same 30 min heat treatment (referred to as N2 induced). Twelve hours after induction, induced *nIs774*, induced N2, as well as uninduced controls of each genotype were collected, washed five times with distilled water and snap frozen in liquid nitrogen. Worms were then thawed in 300 µl TRI reagent (Zymo Research) and lysed using a Qiagen TissueLyser II (5 min, 30 Hz). Following lysis, samples were centrifuged at maximal speed in a table-top centrifuge at 4 °C for 10 min. Total RNA was then extracted using a Direct-zol RNA Miniprep kit (Zymo Research). RNA quality was assessed by determining OD260/280 and OD260/230 ratios using a nanodrop system. PolyA RNAseq libraries were prepared and run on an Illumina NextSeq sequencer by the Michigan Advanced Genomics core.

### RNAseq differential expression analysis

RNA-seq raw read counts received from the UM advanced genomics core were normalized using the GeTMM normalization method.[35] Removal of adapters and quality-control trimming was conducted using fastp.[36] These trimmed reads were aligned and quantified with HISAT2 and featurecounts[37] mouse genome mm39, *C elegans* genome WBcel235.[38] For this, we normalized raw read counts by gene length and used the normalized data as input into edgeR to perform Trimmed Mean of M-values normalization. To perform differential expression analysis, we used the Limma/Voom differential expression pipeline.[39,40] We further used the Benjamini-Hochberg method to control for false positive rates. We choose an adjusted *P* value of 1% for our significance level and a $\log_{10}$-fold change of at least two to determine differentially expressed genes. *C elegans* gene ontology results used the wormbase enrichment analysis tool.[41–43] With the MEF differential expression results, we used ontology enrichment tools such as GSEA[44] and topGO[45] in R.

### STRING network analysis

A list of genes that were at least two-fold up-regulated in the induced *nIs774* cohort compared to the induced N2 wild-type cohort was used as input for a network analysis using STRING (string-db.org).[46] Fold increase in gene transcription was added manually to graphic output using Adobe Illustrator.

### Immunoblotting

Whole-cell protein extracts from MEFs or *C elegans* pellets were prepared in protein sample buffer (62.5 mM Tris pH 6.8, 2% SDS, 10% glycerol). Lysates were sonicated using a Model 120 Sonic Dismembrator (Fisher Scientific) for 20 s set to 30% amplitude. Lysates were then clarified by centrifugation at 15,000 rcf for 15 min at 4ºC. Protein concentrations were determined using DC Protein Assay (Bio-Rad). Equivalent amounts (10 µg) of total protein, supplemented with 710 mM β-mercaptoethanol and 0.01% (w/v) bromophenol blue, then boiled for 5 min, were fractionated by SDS-PAGE on a 12% polyacrylamide gel, electrophoretically transferred to PVDF, and probed with antibodies diluted in 5% nonfat milk or 5% BSA in 1XTBS-0.1% Tween-20. Membranes were imaged on an ImageQuant LAS 4000 Scanner (GE Healthcare) after application of Immobilon Western HRP Substrate (Millipore). Antibodies used in this study were: 17G6 for AMPylation,[47] anti-BiP (for MEFs) Cat#: 66574-1-Ig (Proteintech), anti-BiP (for HSP-3 and HSP-4) Cat#: 11587-1-AP (Proteintech), anti-beta-actin (8H10D10) Cat#: 3700 (Cell Signaling), anti-alpha-tubulin Cat#: 12G10-s (Developmental Studies Hybridoma Bank), anti-FICD Cat#: HPA021390 (Millipore Sigma), anti-HA C29F4 Cat#: 3724 (Cell Signaling), anti-rabbit IgG, HRP linked Cat#: 7074 (Cell Signaling), and anti-mouse IgG, HRP linked Cat# 7064 (Cell Signaling).

### Quantitative RT-PCR

Total RNA was extracted from frozen MEF or *C elegans* pellets in 1 ml of TRIzol reagent (Invitrogen), according to the manufacturer's instructions. To remove contaminating genomic DNA, RNA was incubated with 10 units of RNAse-free DNAse I (Roche) at 37 °C for 30 min presence of 10 units of RNAse inhibitor (Roche). RNA

was then purified using the RNA Clean and Conentrator-5 Kit (Zymo Research). Reverse transcription of 2 μg of cDNA was then carried out at 37°C for 2 h using the High-Capacity cDNA Reverse Transcription kit (Applied Biosystems), according to the manufacturer's instructions. Equivalent amounts of cDNA (10 ng per 10 μl reaction) were cycled in a QuantStudio 6 Pro Real-Time PCR system (ThermoFisher Scientific). Reactions were setup in the presence of 500 nM of each primer in the PowerUp SYBR Green Master Mix (Applied Biosystems) and cycled according to the manufacturer's instructions. Expression analysis was done using the $2^{-dCq}$ formula, normalizing to *Eef-2* for MEF samples and *cdc-42* for *C elegans* samples. Each primer set resulted in a single peak after melting curve analysis, indicating a single product was formed.

**CRediT authorship contribution statement** **Mirella A. Hernandez-Lima:** Writing – review & editing, Investigation, Conceptualization. **Blaise L. Mariner:** Writing – review & editing, Visualization, Software, Methodology, Investigation, Formal analysis, Data curation. **William Giblin:** Writing – review & editing, Investigation, Conceptualization. **Mark A. McCormick:** Writing – review & editing, Conceptualization. **Matthias C. Truttmann:** Writing – review & editing, Writing – original draft, Visualization, Supervision, Project administration, Funding acquisition, Formal analysis, Data curation, Conceptualization.

**Data availability** Data will be made available on request.

**Declaration of interest** The authors declare the following financial interests/personal relationships, which may be considered as potential competing interests: Matthias Truttmann reports financial support was provided by the National Institute of General Medical Sciences. If there are other authors, they declare that they have no known competing financial interests or personal relationships that could have appeared to influence the work reported in this paper.

**Acknowledgments** The authors thank the members of the Truttmann lab for their helpful comments and discussions. MHL is a Rackham fellow and obtained support from NIA Training Grant AG000114, 1F31DC02039701 (Kirschstein NRSA), and 1F99NS135768 (D-SPAN). MCT is supported by grant 1R35GM142561. MAM is supported by NIH R01AG07077601 and a Longevity Impetus Grant. MHL and MCT are responsible for the data presented in this publication. The presented findings are not necessarily representative of the official views of the National Institutes of Health. During the preparation of this work the author(s) used GPT-4.1, GPT-o3, and Claude 4-Sonnet to generate draft figure legends and results sections based on bullet-point-based input. After using these tools/services, the author(s) reviewed and edited the content as needed and take(s) full responsibility for the content of the published article.

## Appendix A. Supporting information

Supplementary data associated with this article can be found in the online version at doi:10.1016/j.cstres.2026.100149.

## References

1. Perera LA, Rato C, Yan Y, et al. An oligomeric state-dependent switch in the ER enzyme FICD regulates AMPylation and deAMPylation of BiP. *EMBO J.* 2019;38:e102177. https://doi.org/10.15252/embj.2019102177
2. Chatterjee BK, Truttmann MC. Fic and non-Fic AMPylases: protein AMPylation in metazoans. *Open Biol.* 2021;11:210009. https://doi.org/10.1098/rsob.210009
3. Casey AK, Orth K. Enzymes involved in AMPylation and deAMPylation. *Chem Rev.* 2018;118:1199–1215. https://doi.org/10.1021/acs.chemrev.7b00145
4. Casey AK, Moehlman AT, Zhang J, et al. Fic-mediated deAMPylation is not dependent on homodimerization and rescues toxic AMPylation in flies. *J Biol Chem.* 2018;293:1550. https://doi.org/10.1074/jbc.AAC118.001798
5. Perera LA, Preissler S, Zaccai NR, et al. Structures of a deAMPylation complex rationalise the switch between antagonistic catalytic activities of FICD. *Nat Commun.* 2021;12:5004. https://doi.org/10.1038/s41467-021-25076-7
6. Preissler S, Rato C, Perera LA, Saudek V, Ron D. FICD acts bifunctionally to AMPylate and de-AMPylate the endoplasmic reticulum chaperone BiP. *Nat Struct Mol Biol.* 2017;24:23–29. https://doi.org/10.1038/nsmb.3337
7. Preissler S, Rohland L, Yan Y, et al. AMPylation targets the rate-limiting step of BiP's ATPase cycle for its functional inactivation. *Elife.* 2017;6. https://doi.org/10.7554/eLife.29428
8. Moehlman AT, Casey AK, Servage K, Orth K, Krämer H. Adaptation to constant light requires Fic-mediated AMPylation of BiP to protect against reversible photoreceptor degeneration. *Elife.* 2018;7. https://doi.org/10.7554/eLife.38752
9. Kielkowski P, Buchsbaum IY, Becker T, et al. A pronucleotide probe for live-cell imaging of protein AMPylation. *Chembiochem.* 2020;21:1285–1287. https://doi.org/10.1002/cbic.201900716
10. Kielkowski P, Buchsbaum IY, Kirsch VC, et al. FICD activity and AMPylation remodelling modulate human neurogenesis. *Nat Commun.* 2020;11:517. https://doi.org/10.1038/s41467-019-14235-6
11. Sanyal A, Chen AJ, Nakayasu ES, et al. A Novel link between Fic (Filamentation induced by cAMP)-mediated Adenylylation/AMPylation and the unfolded protein response. *J Biol Chem.* 2015;290:8482–8499. https://doi.org/10.1074/jbc.M114.618348
12. Ham H, Woolery AR, Tracy C, et al. Unfolded protein response-regulated dFic reversibly AMPylates BiP during endoplasmic reticulum homeostasis. *J Biol Chem.* 2014;289:36059–36069. https://doi.org/10.1074/jbc.M114.612515
13. Preissler S, Rato C, Chen R, et al. AMPylation matches BiP activity to client protein load in the endoplasmic reticulum. *Elife.* 2015;4. https://doi.org/10.7554/eLife.12621
14. Truttmann MC, Cruz VE, Guo X, et al. The *Caenorhabditis elegans* protein FIC-1 Is an AMPylase that covalently modifies heat-shock 70 family proteins, translation elongation factors and histones. *PLoS Genet.* 2016;12:e1006023. https://doi.org/10.1371/journal.pgen.1006023
15. Casey AK, Stewart NM, Zaidi N, et al. FicD regulates adaptation to the unfolded protein response in the murine liver. *Biochimie.* 2024;225:114–124. https://doi.org/10.1016/j.biochi.2024.05.012
16. Gulen B, Kinch LN, Servage KA, et al. FicD sensitizes cellular response to glucose fluctuations in mouse embryonic fibroblasts. *bioRxiv.* 2024. https://doi.org/10.1101/2024.01.22.576705
17. Casey AK, Gray HF, Chimalapati S, et al. Fic-mediated AMPylation tempers the unfolded protein response during physiological stress. *Proc Natl Acad Sci U S A.* 2022;119:e2208317119. https://doi.org/10.1073/pnas.2208317119

18. McCaul N, Porter CM, Becker A, et al. Deletion of mFICD AMPylase alters cytokine secretion and affects visual short-term learning in vivo. *J Biol Chem.* 2021;297:100991. https://doi.org/10.1016/j.jbc.2021.100991
19. Lacy SM, Taubitz RJ, Urban ND, et al. FICD (FIC Domain Protein Adenylyl Transferase) deficiency protects mice from hypertrophy-induced heart failure and promotes BiP (Binding Immunoglobulin Protein) - Mediated Activation of the Unfolded Protein Response and Endoplasmic Reticulum-Selective Autophagy in Cardiomyocytes. *J Am Heart Assoc.* 2025;14:e040192. https://doi.org/10.1161/JAHA.124.040192
20. Truttmann MC, Pincus D, Ploegh HL. Chaperone AMPylation modulates aggregation and toxicity of neurodegenerative disease-associated polypeptides. *Proc Natl Acad Sci U S A.* 2018;115:E5008–E5017. https://doi.org/10.1073/pnas.1801989115
21. Truttmann MC, Zheng X, Hanke L, et al. Unrestrained AMPylation targets cytosolic chaperones and activates the heat shock response. *Proc Natl Acad Sci U S A.* 2017;114:E152–E160. https://doi.org/10.1073/pnas.1619234114
22. Truttmann MC, Wu Q, Stiegeler S, et al. HypE-specific nanobodies as tools to modulate HypE-mediated target AMPylation. *J Biol Chem.* 2015;290:9087–9100. https://doi.org/10.1074/jbc.M114.634287
23. Perera LA, Hattersley AT, Harding HP, et al. Infancy-onset diabetes caused by de-regulated AMPylation of the human endoplasmic reticulum chaperone BiP. *EMBO Mol Med.* 2023;15:e16491. https://doi.org/10.15252/emmm.202216491
24. Rebelo AP, Ruiz A, Dohrn MF, et al. BiP inactivation due to loss of the deAMPylation function of FICD causes a motor neuron disease. *Genet Med.* 2022;24:2487–2500. https://doi.org/10.1016/j.gim.2022.08.019
25. Urban ND, Lacy SM, Van Pelt KM, et al. Functionally diversified Caenorhabditis elegans BiP orthologs control body growth, reproduction, stress resistance, aging, and autophagy. *Nat Commun.* 2025;16:11094. https://doi.org/10.1038/s41467-025-65998-0
26. Singh V, Aballay A. Regulation of DAF-16-mediated innate immunity in *Caenorhabditis elegans*. *J Biol Chem.* 2009;284:35580–35587. https://doi.org/10.1074/jbc.M109.060905
27. Troemel ER, Chu SW, Reinke V, et al. p38 MAPK regulates expression of immune response genes and contributes to longevity in *C. elegans*. *PLoS Genet.* 2006;2:e183. https://doi.org/10.1371/journal.pgen.0020183
28. Calixto A, Chelur D, Topalidou I, Chen X, Chalfie M. Enhanced neuronal RNAi in *C. elegans* using SID-1. *Nat Methods.* 2010;7:554–559. https://doi.org/10.1038/nmeth.1463
29. Sano R, Reed JC. ER stress-induced cell death mechanisms. *Biochim Biophys Acta.* 2013;1833:3460–3470. https://doi.org/10.1016/j.bbamcr.2013.06.028
30. Chen X, Shi C, He M, Xiong S, Xia X. Endoplasmic reticulum stress: molecular mechanism and therapeutic targets. *Signal Transduct Target Ther.* 2023;8:352. https://doi.org/10.1038/s41392-023-01570-w
31. Bult CJ, Sternberg PW. The alliance of genome resources: transforming comparative genomics. *Mamm Genome.* 2023;34:531–544. https://doi.org/10.1007/s00335-023-10015-2
32. Chipurupalli S, Samavedam U, Robinson N. Crosstalk between ER stress, autophagy and inflammation. *Front Med.* 2021;8:758311. https://doi.org/10.3389/fmed.2021.758311
33. Metcalf MG, Higuchi-Sanabria R, Garcia G, Tsui CK, Dillin A. Beyond the cell factory: homeostatic regulation of and by the UPR(ER). *Sci Adv.* 2020;6:eabb9614. https://doi.org/10.1126/sciadv.abb9614
34. Van Pelt KM, Truttmann MC. Loss of FIC-1-mediated AMPylation activates the UPRER and upregulates cytosolic HSP70 chaperones to suppress polyglutamine toxicity. *PLoS Genet.* 2025;21:e1011723. https://doi.org/10.1371/journal.pgen.1011723
35. Smid M, Coebergh van den Braak RRJ, van de Werken HJG, et al. Gene length corrected trimmed mean of M-values (GeTMM) processing of RNA-seq data performs similarly in intersample analyses while improving intrasample comparisons. *BMC Bioinform.* 2018;19:236. https://doi.org/10.1186/s12859-018-2246-7
36. Kim D, Paggi JM, Park C, Bennett C, Salzberg SL. Graph-based genome alignment and genotyping with HISAT2 and HISAT-genotype. *Nat Biotechnol.* 2019;37:907–915. https://doi.org/10.1038/s41587-019-0201-4
37. Liao Y, Smyth GK, Shi W. featureCounts: an efficient general purpose program for assigning sequence reads to genomic features. *Bioinformatics.* 2014;30:923–930. https://doi.org/10.1093/bioinformatics/btt656
38. Mariner BL, Felker DP, Cantergiani RJ, Peterson J, McCormick MA. Multiomics of GCN4-dependent replicative lifespan extension models reveals Gcn4 as a regulator of protein turnover in yeast. *Int J Mol Sci.* 2023;24. https://doi.org/10.3390/ijms242216163
39. Law CW, Chen Y, Shi W, Smyth GK. voom: precision weights unlock linear model analysis tools for RNA-seq read counts. *Genome Biol.* 2014;15:R29. https://doi.org/10.1186/gb-2014-15-2-r29
40. Ritchie ME, Phipson B, Wu D, et al. limma powers differential expression analyses for RNA-sequencing and microarray studies. *Nucleic Acids Res.* 2015;43:e47. https://doi.org/10.1093/nar/gkv007
41. Hu Y, Flockhart I, Vinayagam A, et al. An integrative approach to ortholog prediction for disease-focused and other functional studies. *BMC Bioinform.* 2011;12:357. https://doi.org/10.1186/1471-2105-12-357
42. Angeles-Albores D, RY NL, Chan J, Sternberg PW. Tissue enrichment analysis for *C. elegans* genomics. *BMC Bioinform.* 2016;17:366. https://doi.org/10.1186/s12859-016-1229-9
43. Angeles-Albores D, Lee R, Chan J, Sternberg P. Two new functions in the WormBase Enrichment Suite. *MicroPubl Biol.* 2018;2018. https://doi.org/10.17912/W25Q2N
44. Subramanian A, Tamayo P, Mootha VK, et al. Gene set enrichment analysis: a knowledge-based approach for interpreting genome-wide expression profiles. *Proc Natl Acad Sci U S A.* 2005;102:15545–15550. https://doi.org/10.1073/pnas.0506580102
45. Alexa AR, J. Gene set enrichment analysis with topGO. 2016. https://www.bioconductor.org/packages//2.7/bioc/vignettes/topGO/inst/doc/topGO.pdf.
46. Szklarczyk D, Gable AL, Lyon D, et al. STRING v11: protein-protein association networks with increased coverage, supporting functional discovery in genome-wide experimental datasets. *Nucleic Acids Res.* 2019;47:D607–D613. https://doi.org/10.1093/nar/gky1131
47. Hopfner D, Fauser J, Kaspers MS, et al. Monoclonal Anti-AMP antibodies are sensitive and valuable tools for detecting patterns of AMPylation. *iScience.* 2020;23:101800. https://doi.org/10.1016/j.isci.2020.101800